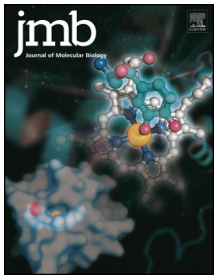

Cysteine-Independent Inhibition of Alzheimer's Disease-like Paired Helical Filament Assembly by Leuco-Methylthioninium (LMT)

Youssra K. Al-Hilaly[1,2], Saskia J. Pollack[1], Janet E. Rickard[3], Michael Simpson[4,5], Ana-Caroline Raulin[1], Thomas Baddeley[4,5], Pascale Schellenberger[1], John M.D. Storey[4,5], Charles R. Harrington[3,5], Claude M. Wischik[3,5] and Louise C. Serpell[1]

*1 - **Dementia Research Group,** School of Life Sciences, University of Sussex, Falmer, E Sussex, BN1 9QG, United Kingdom*
*2 - **Chemistry Department,** College of Science, Mustansiriyah University, Baghdad, Iraq*
*3 - **Institute of Medicine,** Medical Sciences and Nutrition, University of Aberdeen, Aberdeen, AB25 2ZP, United Kingdom*
*4 - **TauRx Therapeutics Ltd.,** Aberdeen, AB25 2ZP, United Kingdom*
*5 - **Department of Chemistry,** University of Aberdeen, Aberdeen, AB24 3UE, United Kingdom*

***Correspondence to Claude M. Wischik and Louise C. Serpell:** C.M. Wischik is to be contacted at: Institute of Medicine, Medical Sciences and Nutrition, University of Aberdeen, Aberdeen, AB25 2ZP, United Kingdom. cmw@taurx.com; L.C.Serpell@sussex.ac.uk*
https://doi.org/10.1016/j.jmb.2018.08.010
Edited by Sheena Radford

Abstract

Alzheimer's disease is a tauopathy characterized by pathological fibrillization of tau protein to form the paired helical filaments (PHFs), which constitute neurofibrillary tangles. The methylthioninium (MT) moiety reverses the proteolytic stability of the PHF core and is in clinical development for treatment of Alzheimer's disease in a stable reduced form as leuco-MT. It has been hypothesized that MT acts *via* oxidation of cysteine residues, which is incompatible with activity in the predominantly reducing environment of living cells. We have shown recently that the PHF-core tau unit assembles spontaneously *in vitro* to form PHF-like filaments. Here we describe studies using circular dichroism, SDS-PAGE, transmission electron microscopy and site-directed mutagenesis to elucidate the mechanism of action of the MT moiety. We show that MT inhibitory activity is optimal in reducing conditions, that the active moiety is the reduced leuco-MT form of the molecule and that its mechanism of action is cysteine independent.

Introduction

Tau protein plays a role in the assembly and stability of microtubules in the cytoplasm [1–3] and in the stabilization of heterochromatin in the nucleus [4]. Tau is encoded by the *MAPT* gene on chromosome 17 and alternative splicing generates six major isoforms of tau in the central nervous system, three with four imperfect repeat regions and three with three repeats. In Alzheimer's disease (AD) and a group of neurodegenerative diseases, known collectively as tauopathies, tau accumulates abnormally in the brain. In AD, tau protein self-assembles to form paired helical filaments (PHFs) and straight filaments that constitute the neurofibrillary tangles within neurons and dystrophic neurites in brain. The tau species isolated from proteolytically stable PHF-core preparations from AD brain tissue comprise a mixture of fragments derived from both three- and four-repeat isoforms, but restricted to the equivalent of three repeats, with an N-terminus at residues Ile-297 or His-299 (four-repeat numbering) and the C-terminus at residue Glu-391, or at homologous positions in other species [5,6]. The same segment of the molecule, encompassing residues 306–378, has been confirmed as constituting the core of the PHF using cryo-electron microscopy analysis of PHFs extracted from AD brain tissue [7] and a homologous core

fragment from three-repeat tau has been identified in the filaments found in some forms of frontotemporal dementia [8].

Since tau aggregation pathology is closely associated with cognitive decline [9–18], treatment based on the use of tau aggregation inhibitors offers a potentially promising therapeutic approach for AD [19]. We have shown previously that the methylthioninium (MT) moiety, which can exist in oxidized (MT^+, Fig. 1a) and reduced leuco-MT (LMT; Fig. 1b) forms, is able to act as a tau aggregation inhibitor in cell-free [20,21], cell-based [20] and tau transgenic mouse models of tau aggregation [22]. When applied to preparations of proteolytically stable PHFs isolated from AD brain, MT reverses the proteolytic stability of the constituent tau protein [21] at protein/MT molar ratios upward of approximately 1:0.1 [20].

Attempts to understand the mechanism of action of the MT moiety have been based so far on heparin-induced filament formation using the repeat-domain tau fragments known as K19 and K18 [23]. Heparin-induced filaments formed by tau are highly heterogeneous structures that differ from AD PHFs [24]. The three-repeat K19 fragment, which is nearest to the core tau unit of the PHF, encompasses repeats R1, R3 and R4 (Gln-244–Glu-372, without R2). It includes the additional R1 at the N-terminus which is not present in PHF core tau unit isolated from AD brain tissues [25] or in the protein used in the present studies. When included during heparin-induced assembly of the K19 fragment (which contains a single cysteine at 322), the MT moiety has been reported to produce an intermolecular disulfide cross-linked dimer in non-reducing (but not in reducing) conditions [23]. Such dimers have been shown to enhance filament formation, and this has been taken to be the explanation for the relative lack of inhibitory effect of MT on K19 fibrillization in either oxidizing or reducing conditions [23]. The K18 fragment containing repeats R1, R2, R3 and R4 differs even more from the PHF core tau unit, with an extra 54 residues at the N-terminus relative to the PHF core tau unit and contains two cysteine residues. The MT moiety inhibits heparin-induced fibrillization of the K18 fragment only in non-reducing conditions, and this effect requires formation of an intramolecular disulfide cross-link that renders the K18 peptide assembly incompetent [23]. Therefore, it has been hypothesized that the mechanism of tau aggregation inhibition by the MT moiety is *via* cysteine oxidation [23,26].

We have reported recently that the truncated tau fragment corresponding to one of the species isolated from proteolytically stable PHF preparations (residues Ile-297–Glu-391) and referred to as "dGAE" [25,27] has quite different assembly properties *in vitro* from those reported using K19 and K18 fragments. The dGAE fragment does not require heparin to induce fibrillization. It assembles spontaneously in physiological conditions *in vitro* into filaments that closely resemble native PHFs and straight filaments from AD brain morphologically [28]. These *in vitro* assembled PHFs display a characteristic β-sheet structure by circular dichroism (CD) and X-ray fiber diffraction analysis. Previous studies, using a 1–383 tau fragment, have suggested that heparin-induced assembly is enhanced

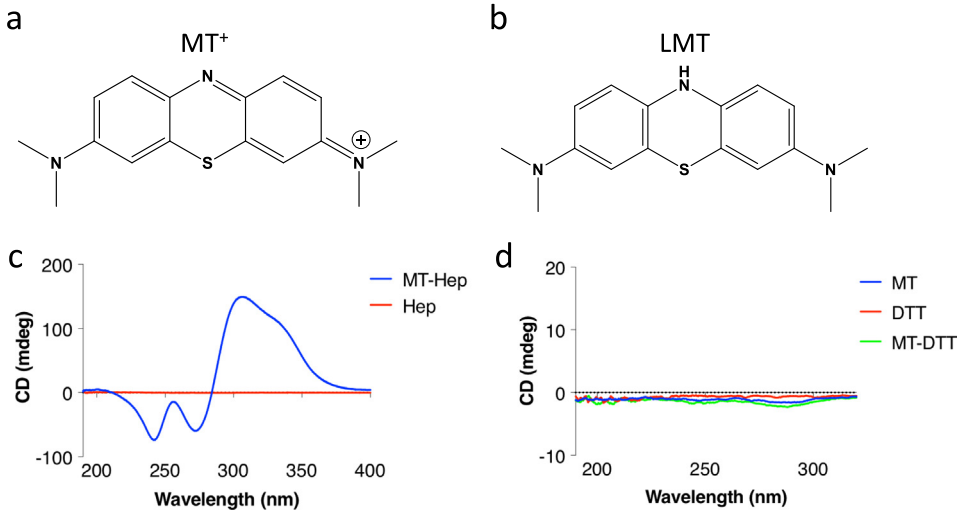

Fig. 1. Chemical structures of (a) MT and (b) LMT and CD spectra for MT with heparin and DTT. (c) CD spectra for heparin (0.034 mg/ml) with or without MT (0.33 mM) showing strong CD signals arising from ordering of the MT with heparin (d) CD spectra for MT (0.5 mM) incubated with and without DTT (10 mM) in 10 mM phosphate buffer (pH 7.4) for 24 h at 37 °C with 700 oscillations per minute of agitation in the dark. No CD signal arose from MT alone, DTT alone, or MTC plus DTT. CD spectra were collected using a 0.02-cm path length cuvette.

by disulfide formation and reduced by the substitution of Cys322Ala [29]. However, in contrast to the behavior of the K19, K18 and 1–383 fragments *in vitro*, dGAE filament assembly is substantially enhanced in reducing conditions, or with replacement of the single cysteine residue at position 322 with alanine. This suggests that the assembly of the PHF core tau unit is unrelated to cysteine cross-linking and calls into question the cysteine oxidation hypothesis as the explanation of the mechanism of action of the MT moiety. We have applied a range of structural approaches aiming to understand the mechanism of action of the MT moiety as this applies to the PHF core tau unit. We show that inhibitory activity is optimal in reducing conditions, that the active moiety responsible for inhibition of tau aggregation is the reduced LMT form of the molecule and that the mechanism of action is cysteine-independent. A stable reduced form of MT (leuco-methylthioninium bis(hydromethanesulfonate), "LMTM," USAN name "hydromethylionine mesylate") is currently in phase 3 clinical development for treatment of AD and frontotemporal dementia.

Results

Heparin binds directly to the MT moiety

Heparin has been used previously to study the mechanism of action of the MT moiety [23,26]. A CD spectrum of MT incubated with heparin at a heparin/MT molar ratio of 1:3 is shown in Fig. 1c. A very prominent and broad CD peak was observed at 300 and 340 nm that was absent when either heparin or MT was incubated alone (Fig. 1c and d). This peak therefore arises as a result of an association between the MT moiety and heparin.

dGAE assembly in the presence of MT in non-reducing conditions

dGAE assembles spontaneously into filaments without a requirement for heparin [28]. When MT was included during dGAE assembly in non-reducing conditions at tau/MT ratios ranging from 1:0.1 to 1:10, CD spectra showed an increased random coil content (minimum shown at 200 nm) in the supernatant (Fig. 2b) and a corresponding reduction in fibrillar β-sheet structure in the pellet (red-shifted minimum at 230 nm [28] (Fig. 2a). The appearance of a red-shifted peak for β-sheet is commonly observed for elongated β-sheets that appear in amyloid fibrils [30,31]. In addition, a new CD peak at 300 nm, with an accompanying shoulder at 250 nm, appeared in the pellet fraction (Fig. 2a). To explore the origin of this new peak, CD spectra were collected on the pellet of centrifuged preformed fibrils (prepared in non-reducing conditions) before and immediately after MT was added. The spectra showed reduction of the signal at 230 nm and a very weak, broad maximum at 280–300 nm (Fig. S1).

In the absence of MT, Coomassie-stained SDS-PAGE gels showed the presence of species with 10- and 12-kDa mobilities in the supernatant and that the bulk of the protein sedimented in a low-speed pellet that was dominated by a dimer having gel mobility of 24 kDa, as well as a 12-kDa monomer and a 48-kDa oligomer [28]. When assembly was conducted in the presence of MT, there was a slight reduction in the 12- and 24-kDa species in the pellet at a tau/MT molar ratio of 1:0.2, although generally the intensity of bands remained similar for increasing ratios of MT (Fig. 2c).

There was no clear effect of the MT moiety on the appearance of the short filaments assembled in non-reducing conditions by TEM. Clumping of short filaments into large fibrillar aggregates and some elongated filaments became apparent at high molar ratios (1:5 and 1:10; Fig. 2d).

dGAE assembly in the presence of MT in reducing conditions

We have shown previously that assembly of dGAE is substantially enhanced in reducing conditions (DTT, 10 mM) [28]. In order to examine the effect of MT during assembly in reducing conditions, we first showed that the CD spectrum of MT itself was unaffected by the presence of DTT (Fig. 1d). Using a combination of UV spectroscopy and mass spectrometry, we showed that the predominant MT species present in the reducing conditions used is the reduced form, LMT. By contrast, the predominant species in non-reducing conditions is the oxidized form, MT^+ (Fig. S2a). UV spectrometry showed the presence of MT^+ in the absence of DTT, with a prominent absorbance peak at 600 and 680 nm as well as a peak at 300 nm. DTT alone gave a strong peak at 200–210 nm (Fig. S2a, b). DTT with MT resulted in a sharp peak at approximately 250 nm with a small shoulder at 300 nm (Fig. S2a). The MT^+-specific peak at 600–680 was absent, showing that under reducing conditions, most of the MT is present as LMT. Mass spectrometry confirmed the presence of MT^+ following ionization (Fig. S2d).

dGAE assembly in the presence of MT under reducing conditions resulted in a clear concentration-dependent loss of β-sheet signal in the CD spectrum of the pellet and a corresponding increase in random coil in the supernatant (Fig. 3a and b). The 300/250-nm peaks were more evident in the CD spectrum from the pellet and were maximal at a tau/MT molar ratio of 1:0.2, decreasing at higher molar ratios (Fig. 3a, b). CD spectra taken when MT was added briefly to the pellet *after* filament assembly showed that the 300/250-nm peaks were more prominent in reducing than in non-reducing conditions (Fig. S2b).

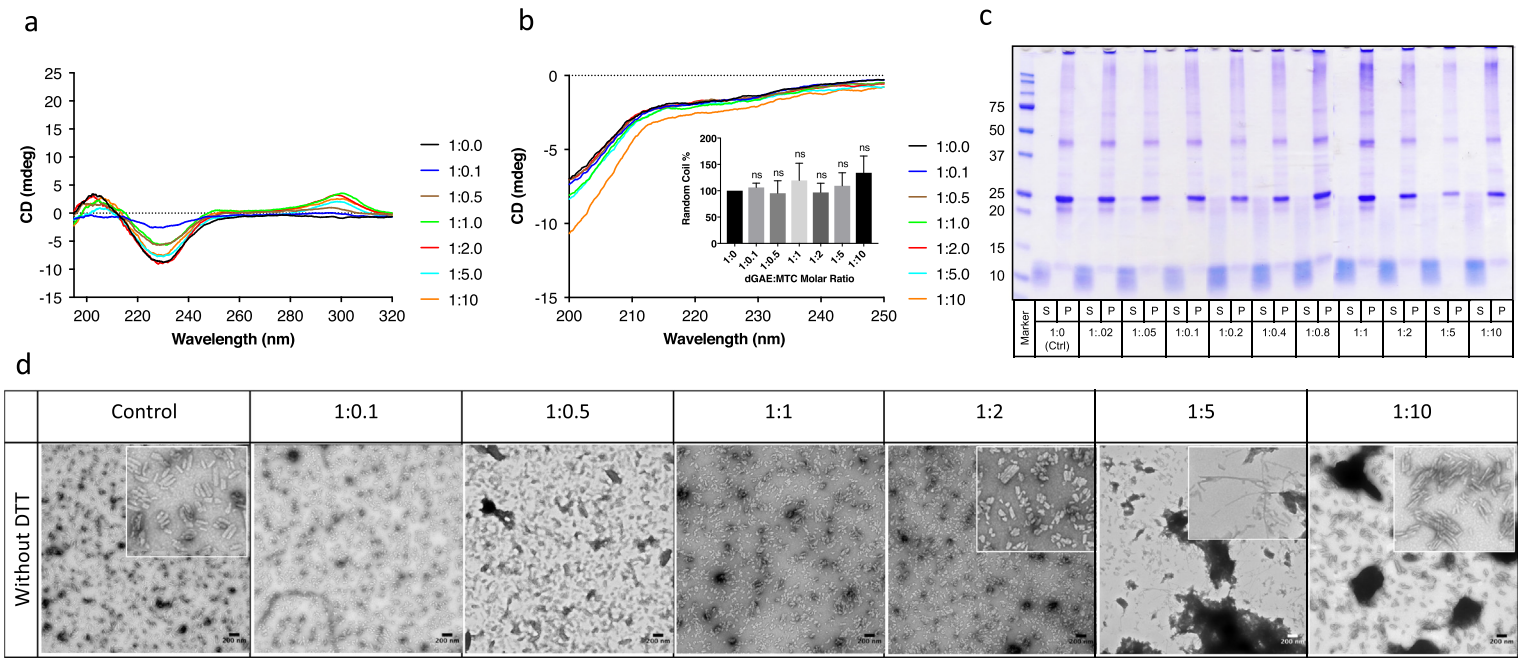

Fig. 2. MT-treated dGAE under non-reducing conditions. dGAE (100 μM) was incubated with MT at different molar ratios in phosphate buffer (10 mM; pH 7.4) for 24 h at 37 °C, with agitation at 700 rpm in the dark. At 24-h incubation, the samples were separated by centrifugation for 15 min at 4 °C and 20,000*g*. CD spectra for the pellet (a) and for the supernatant (b); inset shows a graphical representation of relative intensity at 200 nm against dGAE/MT ratio where 1:0 intensity is 100%. (c) Coomassie-stained gel of non-reducing SDS-PAGE of separated supernatant (S) and pellets (P) at dGAE/MT ratios as shown. (d) Transmission electron micrographs of negatively stained dGAE (100 μM) incubated for 24 h at 37 °C with MT at different molar ratios for dGAE/MT, in the absence of DTT from 0 h. The scale bars represent 200 nm.

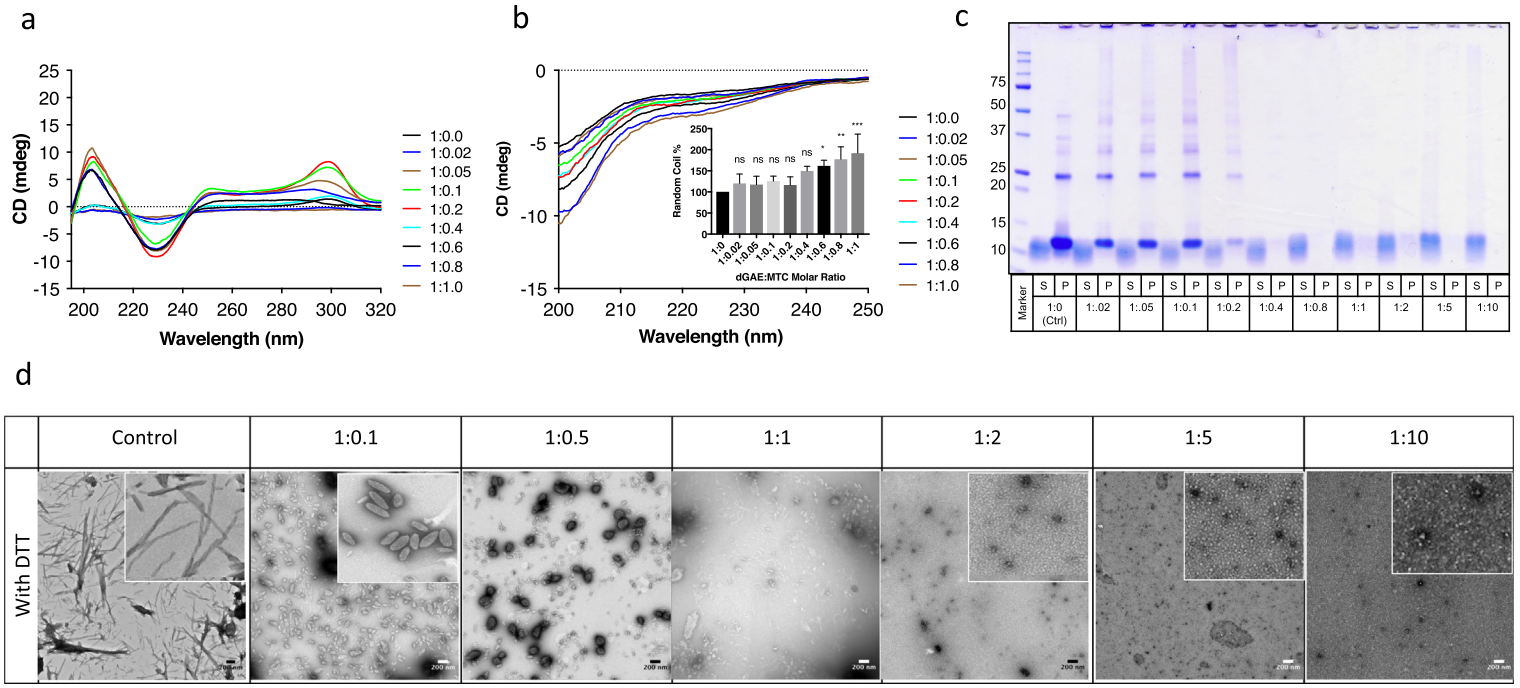

Fig. 3. MT-treated dGAE under reducing conditions. dGAE (100 μM) was incubated with MT using different molar ratios in the presence of 10 mM DTT in 10 mM phosphate buffer (pH 7.4) for 24 h at 37 °C and with 700 oscillations per minute of agitation in the dark. After 24-h incubation, the samples were centrifuged for 15 min at 4 °C and 20,000*g*. The CD spectra were recorded for both (a) pellet and (b) supernatant; inset shows a graphical representation of relative intensity at 200 nm against dGAE/MT ratio where 1:0 intensity is 100%. (c) Coomassie blue-stained, non-reducing SDS-PAGE gel of separated supernatant (S) and pellet (P) fractions of dGAE (100 mM) incubated with different ratios of dGAE/MT as shown. (d) Transmission electron micrographs of negatively stained dGAE (100 μM) incubated for 24 h at 37 °C with MT at different molar ratios for dGAE/MT, in the presence of DTT (10 mM) from 0 h. The scale bars represent 200 nm.

Coomassie-stained gels of dGAE incubated with MT under reducing conditions during assembly showed a marked loss of protein in the pellet at tau/MT molar ratios greater than 1:0.1, with elimination of the predominant 12-kDa monomeric species from the pellet, and transfer to the supernatant. At above 1:0.1 molar ratio, the 24- and 48-kDa species became weak and then absent from both pellet and supernatant (Fig. 3c).

At the threshold molar ratio of 1:0.1, distinctive oval structures were observed by TEM. Interestingly, these oval particles were generally seen only in samples that also produced the 300/250-nm CD peaks. As the concentration of MT was increased, these oval structures disappeared, and the only structures evident on the grid were small spherical particles (Fig. 3d). At higher magnification, the small spherical particles were amorphous in appearance, ranging 2–20 nm in size. In order to characterize them further, single-particle analysis was used to classify particles formed at a tau/MT ratio of 1:5 under reducing conditions. Single-particle averaging revealed that the assemblies fitted into at least 11 distinct morphological classes, but heterogeneity of the samples did not allow for further structural analysis (Fig. S3).

X-ray fiber diffraction was used to investigate whether MT at low concentrations altered the molecular architecture of the filaments. Filament formation was entirely prevented above a tau/MT molar ratio of 1:0.6. At lower ratios (1:0.1, 1:0.2), the diffraction patterns were similar to those reported previously for untreated filaments [28]. At 1:0.4, it was possible to obtain a diffraction film in which there was good alignment of the remaining filaments. These produced meridional and equatorial diffraction signals at 4.7 and 9.5 Å indicating retention of the underlying cross-β architecture (Fig. S4).

Assembly of the dGAE-C322A variant in the presence of MT in non-reducing conditions

We have shown previously that the dGAE-C322A variant lacking cysteine has a greater propensity to form PHFs than the native form [28]. As with the native form, the variant incubated in non-reducing conditions in the presence of MT showed an MT concentration-dependent reduction in β-sheet in the CD spectrum from the pellet accompanied by concentration-dependent peaks at 300/250 nm, which were maximal at a dGAE-C322A/MT molar ratio of 1:5. The CD spectrum of the supernatant showed weak random coil signal, which did not change with increasing concentrations of MT (Fig. 4a, b).

The corresponding SDS-PAGE gels showed that the protein was present predominantly in the pellet as a species with 12-kDa mobility, with a small amount of dimer migrating at 24 kDa. As shown previously [28], the species remaining in the supernatant had a gel mobility of 10 kDa. As the concentration of MT increased, there was more 12- and 24-kDa material in the pellet, as well as the appearance of higher order oligomers (Fig. 4c).

TEM showed the presence of the same oval particles and filaments seen with the native form in the presence of MT at all protein/MT molar ratios (1:0.1–1:5.0) in non-reducing conditions. Higher-magnification TEM showed that the particles were again composed of short, tightly packed filaments. Increasing the concentration of MT produced further aggregation and elongation of the oval particles (Fig. 4d).

Assembly of the dGAE-C322A variant in the presence of MT in reducing conditions

Following assembly of the dGAE-C322A variant in reducing conditions without MT, the CD spectrum of the pellet showed the characteristic β-sheet peak at 205 nm and a shifted trough at around 230 nm [28]. When MT was present during assembly, there was a marked reduction in the β-sheet peak in the material in the pellet and a corresponding increase in random coil in the material remaining in the supernatant. Unlike the native form, there were minimal 250- and 300-nm peaks in the pellet after 24 h (Fig. 5a, b). However, when MT was added briefly to the pellet from preformed dGAE-C322A filaments (Fig. S1d), the 300-nm peak was more intense than in a similar preparation in non-reducing conditions (Fig. S1c).

The corresponding SDS-PAGE gels showed a biphasic transition. Without MT, the majority of protein (at 12 and 24 kDa) was found in the pellet. At a protein/MT molar ratio of 1:0.1, there was increased protein in the supernatant. The protein remaining in the pellet migrated at 12 kDa, with an accompanying regular ladder extending to 60 kDa in multiples of 12 kDa. At higher molar ratios of MT, the pellet was largely eliminated with protein transferred to the supernatant. The supernatant species had the 12-kDa mobility normally associated with sedimenting fractions [28] (Fig. 5c).

dGAE-C322A forms PHF-like filaments in the presence of DTT very similar to those in non-reducing conditions [28]. The major structures found by TEM at a protein/MT molar ratio of 1:0.1 were the oval particles (Fig. 4d). Given their unusual appearance, they were examined further by immunogold TEM using an antibody against total tau to confirm that these assemblies are composed of tau protein and are not artefacts. The short closely packed fibrils were immunoreactive with a tau antibody that did not show any non-specific decoration of amyloid-β (1–42) fibrils (Fig. S5). At higher molar ratios, only the small spherical particles ranging in size from 2 to 20 nm were observed. These are similar to those formed by native dGAE in the presence of MT (Fig. 4d).

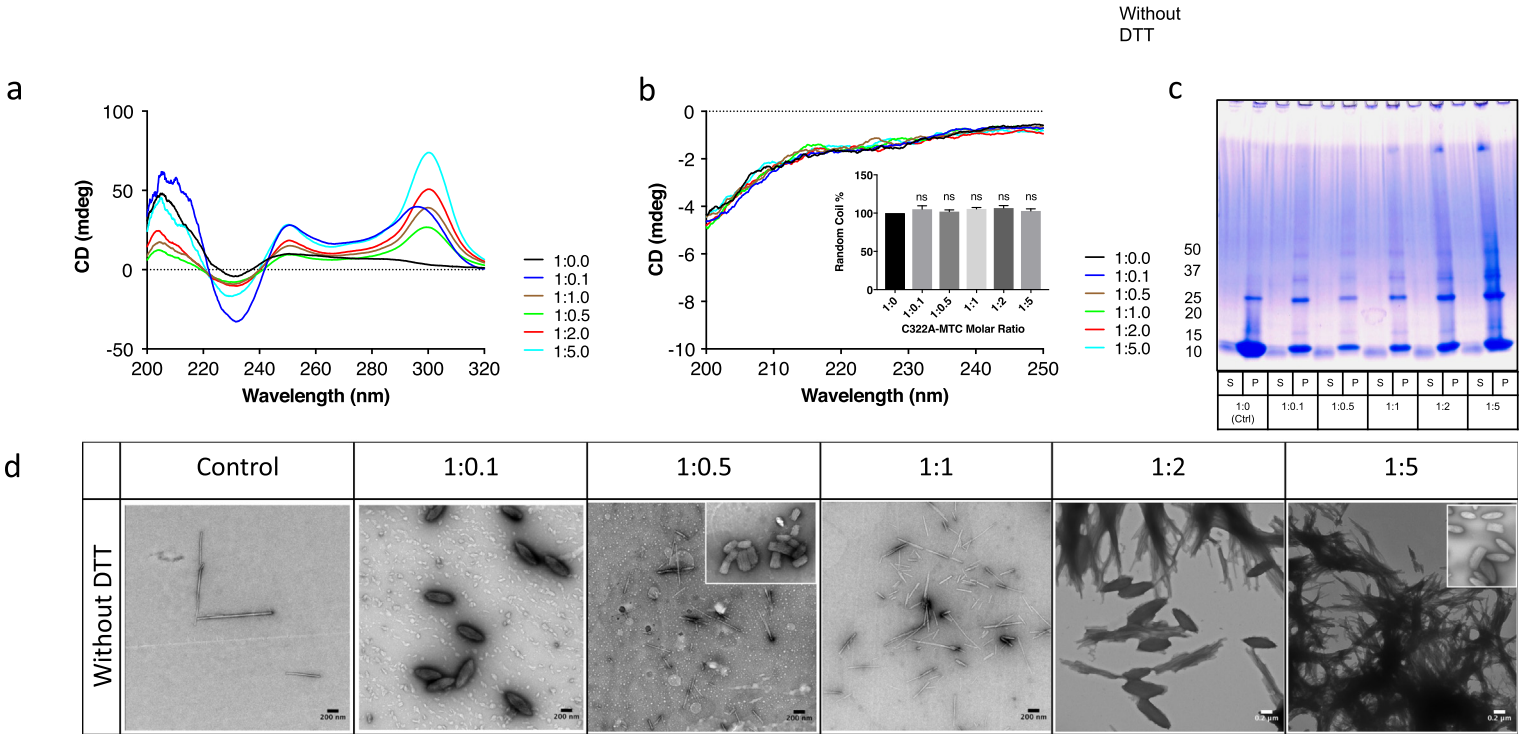

Fig. 4. Inhibition of assembly of dGAE-C322A in non-reducing conditions. C322A variant (100 μM) was incubated with MT using different molar ratios in the absence of 10 mM DTT in 10 mM phosphate buffer (pH 7.4) for 24 h at 37 °C and with 700 oscillations per minute of agitation in the dark. After 24-h incubation, the samples were centrifuged for 15 min at 4 °C and 20,000*g*. The CD spectra were recorded for both (a) pellet and (b) supernatant; inset shows a graphical representation of relative intensity at 200 nm against dGAE/MT ratio where 1:0 intensity is 100%. (c) Coomassie blue-stained, non-reducing SDS-PAGE gel of separated supernatant (S) and pellet (P) fractions of dGAE (100 mM) incubated with different ratios of dGAE/MT as shown. (d) Transmission electron micrographs of negatively stained dGAE (100 μM) incubated for 24 h at 37 °C with MT at different molar ratios for dGAE/MT, in the absence of DTT from 0 h. The scale bars represent 200 nm.

Discussion

We have reported recently that dGAE, the core tau unit of the PHF (residues 297–391), assembles spontaneously *in vitro* into filaments that closely resemble native PHFs morphologically [28]. Spontaneous fibrillization occurs in physiological conditions and without exogenous polyanionic reagents. These synthetic PHFs display a characteristic β-sheet structure by CD and fiber X-ray diffraction analysis. Reducing conditions enhance the assembly of dGAE into PHFs. A cysteine-to-alanine variant also self-assembles to form PHFs, indicating that disulfide cross-linking is unnecessary for filament assembly [28]. We now reveal that the MT moiety is significantly more effective in blocking PHF assembly under reducing conditions. CD spectra showed a dose-dependent reduction in the generation of β-sheet secondary structure in a low-speed pellet and a corresponding increase in random coil in the supernatant. SDS-PAGE gels showed a dose-dependent reduction in protein in the pellet and a transfer to the supernatant. Finally, filaments observed using TEM were eliminated and replaced by a population of small spherical particles. These effects were seen using both wild-type dGAE and the C322A variant. Therefore, the inhibitory effect of the MT moiety on the fibrillization of the PHF core tau unit is not mediated *via* cysteine oxidation.

When MT was incubated with dGAE under non-reducing conditions, the effect was partial. Although there was a dose-dependent reduction in β-sheet in the pellet and a corresponding increase in random coil in the supernatant, this was not associated with a transfer of protein from pellet to supernatant. On SDS-PAGE gels, the 12-kDa monomer and higher-order oligomers became more prominent in the pellet with increasing concentrations of MT, particularly for the C322A variant. There was no clear effect of MT on the appearance of filaments seen by electron microscopy. The effect of MT on assembly in non-reducing conditions was largely the same whether the native dGAE fragment or the C322A variant was used. These results show that inhibition of PHF assembly by the MT moiety requires reducing conditions for optimal efficacy.

The question arises therefore whether the enhancement of the inhibitory effect of MT in reducing conditions is due to an effect on the dGAE species decreasing its propensity to fibrillize, or an effect on the MT moiety. As noted above, dGAE filament assembly is facilitated in reducing conditions. Therefore, reducing conditions must enhance the inhibitory efficacy of the MT moiety itself. The MT moiety can exist in oxidized (MT^+) or reduced (LMT) forms depending on the pH and reducing potential of the milieu. DTT is available in 10- to 100-fold molar excess relative to MT in the reducing conditions used, and we have confirmed by a combination of UV spectroscopy and mass spectrometry that the LMT form is the major species present in these conditions. We conclude, therefore, that LMT is the active moiety required for inhibition of aggregation of the PHF-core tau unit and that it does so in a cysteine-independent manner.

We have shown previously that the dGAE monomer exists in two different conformations with mobilities of 12 or 10 kDa on SDS-PAGE gels. Only the 12-kDa species is assembly competent as it is selectively enriched in the pellet fraction, whereas the 10-kDa species remains in the supernatant where it retains a random coil conformation. These gel mobility and differential sedimentation properties are independent of the cysteine residue at position 322 and are not altered by introducing DTT during assembly. As described in greater detail previously [28], PHFs assembled *in vitro* have the same detailed morphological features as PHFs isolated from AD brain tissue, implying that they are assembled from a similar underlying C-shaped subunit. This C-shaped subunit has been elucidated as a folded hairpin configuration of PHF-core tau unit in AD PHFs [7]. This suggests that the distinctive 12-kDa gel mobility of the assembly-competent unit reflects the same folded hairpin conformation. Since it is specifically this species that is transferred to the supernatant when assembly is conducted in the presence of LMT, the inhibitory effect appears to interfere with the assembly competence of the core tau hairpin rather than conversion to the 10-kDa form. Further immunochemical and computational chemistry studies are required to determine the structural basis of this change in assembly competence.

The present findings shed some further light on the mechanism of LMT inhibition of PHF assembly. We show that an intermediate tau-LMT complex is formed at the threshold molar ratio of 1:0.1, which is insufficient to block PHF assembly completely, but gives rise instead to an oval particle consisting of short, closely packed tau fibrils. These oval particles are associated with the appearance of new MT-dependent CD peaks at 300/250 nm. When MT was added briefly following filament assembly, the 300/250-nm peaks were more evident in reducing than in non-reducing conditions. These findings indicate that LMT rapidly forms a concentration-dependent complex with the core tau unit, which at tau/MT molar ratios greater than 1:0.1 renders it assembly incompetent. This association appears to have greater inhibitory efficacy if the tau unit lacks a cysteine residue at position 322. In contrast to evidence from TEM and SDS-PAGE gels of supernatant and pellet fractions, the MT moiety was able to interfere with the β-sheet CD signal in the pellet in all the conditions studied. Insofar as the β-sheet signal originates from hairpin stacking, this suggests that the MT moiety is able to form an association sufficient to disturb this even in non-reducing conditions. However, this association is not sufficient

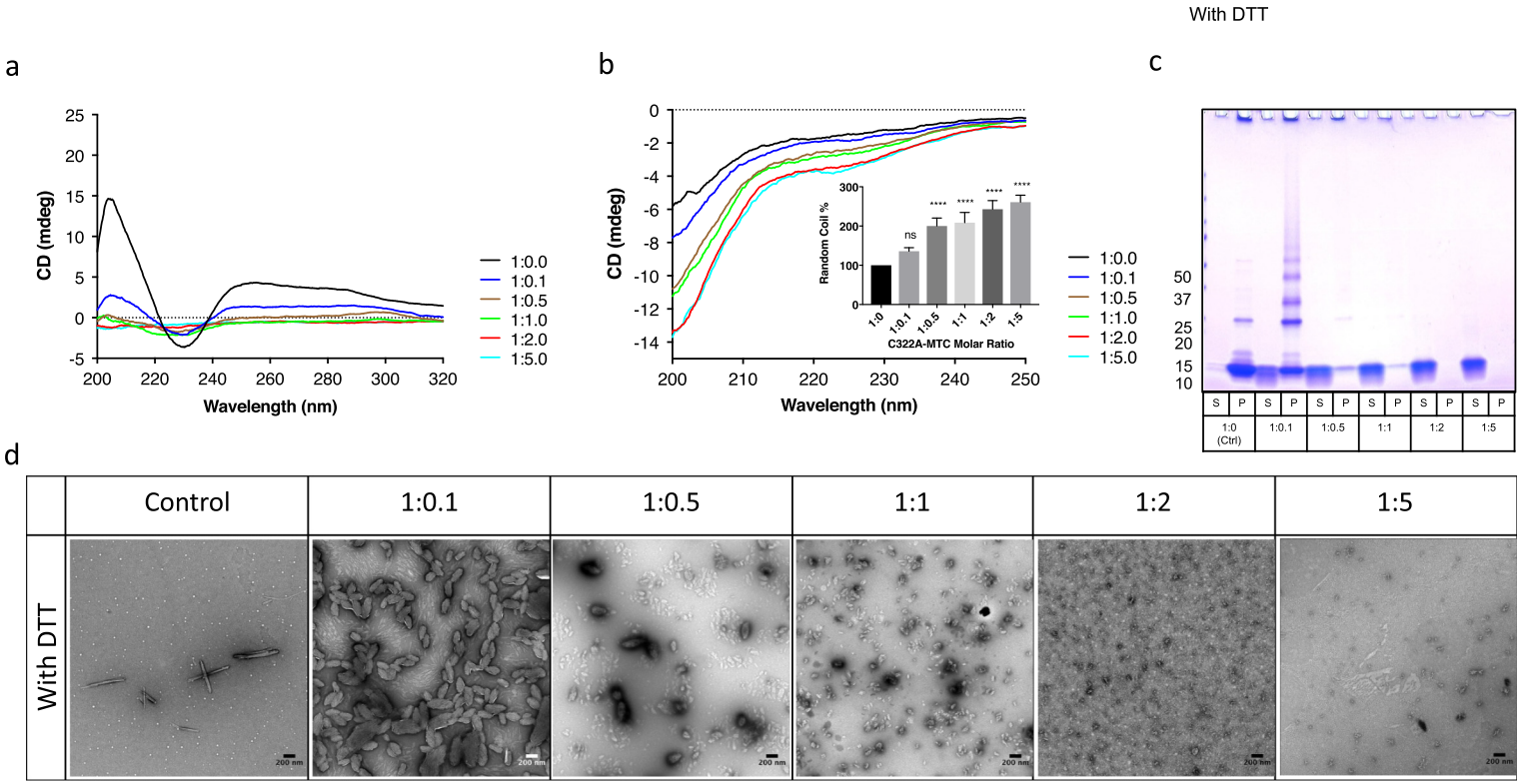

Fig. 5. Inhibition of assembly of dGAE-C322A by MT in reducing conditions. C322A variant (100 μM) was incubated with MT using different molar ratios in the presence of 10 mM DTT in 10 mM phosphate buffer (pH 7.4) for 24 h at 37 °C and with 700 oscillations per minute of agitation in the dark. After 24-h incubation, the samples were centrifuged for 15 min at 4 °C and 20,000*g*. The CD spectra were recorded for both (a) pellet and (b) supernatant; inset shows a graphical representation of relative intensity at 200 nm against dGAE/MT ratio where 1:0 intensity is 100%. (c) Coomassie blue-stained, non-reducing SDS-PAGE gel of separated supernatant (S) and pellet (P) fractions of dGAE (100 mM) incubated with different ratios of dGAE/MT as shown. (d) Transmission electron micrographs of negatively stained dGAE (100 μM) incubated for 24 h at 37 °C with MT at different molar ratios for dGAE/MT, in the presence of DTT (10 mM) from 0 h. The scale bars represent 200 nm.

in the absence of an adequate concentration of LMT to prevent PHF assembly and redistribute protein into the supernatant.

Our results are at odds with the findings from studies based on heparin-induced fibrillization of repeat-domain tau fragments known as K19 and K18. The dGAE core tau unit is the product of a specific tau-tau association that templates truncation, which reproduces the proteolytically stable unit in a prion-like fashion [19,21]. The K19 fragment does not conform to this template and its assembly properties are quite different from those of the PHF-core tau unit. Most notably, there is a 60% reduction in tau aggregation in reducing conditions, and the further inhibitory effect of the MT moiety in these conditions is minimal and evident only at a protein/MT ratio of 1:100 [26]. NMR evidence of a cysteine-dependent association between the MT moiety and full-length tau in a random coil configuration between residues 280 and 330 in non-reducing conditions is also unlikely to have relevance to the cysteine-independent inhibitory effects we describe. Likewise, the fact that inhibitory activity is evident in the absence of a cysteine residue implies that intramolecular disulfide link formation within the K18 fragment is also irrelevant to understanding the mechanism of action of the MT moiety on PHFs [23,26]. More generally, our results suggest that the use of the heparin-induced filament assembly model as a basis for discovering novel tau aggregation inhibitors may produce misleading results.

Although we have used spontaneous assembly of the truncated PHF-core unit as a model system to understand better the mechanism of action of the MT moiety, this should not be taken as implying that tau protein is truncated prior to aggregation. Indeed, we have shown in previous work that the key assembly events are likely to occur in a context of phase asymmetry as regards solid and aqueous phases and that these most likely involve the capture of full-length tau from aqueous phase [19,32]. We have also shown that a prior high-affinity binding interaction through the repeat domain defines the proteolytically stable footprint that corresponds to the PHF-core tau unit [20,21].

On the basis of the cysteine oxidation hypothesis derived from results using the K19 and K18 fragments *in vitro*, Crowe and colleagues [23] argue that MT would be predicted to be relatively ineffective as a tau aggregation inhibitor *in vivo* because its effect is blunted in a reducing environment. Our results, on the contrary, demonstrate that the MT moiety is optimally effective in a reducing environment. We have shown previously that the MT moiety is effective as a tau aggregation inhibitor both in cells and in transgenic mouse models [20,22]. The molar ratio at which the MT moiety becomes effective as an inhibitor of PHF assembly, namely 1:0.1, is approximately the same as that required to reverse the proteolytic stability of PHFs isolated from AD brain tissues [20,21]. The evidence we have presented showing that LMT is the active moiety at the site required for inhibition of aggregation of the core tau unit of the PHF may be part of the explanation for the clinical evidence, suggesting that the stable reduced form of the MT moiety (LMTM, hydromethylthioninium mesylate) appears to be effective at a dose 20-fold lower than the minimum effective dose previously identified using the oxidized MT^+ form [19,33]. A global clinical trial is currently ongoing which aims to confirm that LMTM monotherapy at a dose of 8 mg/day is effective in delaying the progression of early AD.

Materials and Methods

Truncated tau (dGAE) preparation

Recombinant truncated dGAE tau and dGAE-C322A were expressed in bacteria and purified by P11 phosphocellulose chromatography as described previously [21,34], with minor modifications. In some cases, 2-(N-morpholino)ethanesulfonic acid (MES) (pH 6.25) was used instead of piperazine-N,N'-bis(ethanesulfonic acid) (PIPES) and the protein was heat treated [35] instead of DE52 ion-exchange treatment prior to P11 chromatography. Protein fractions were eluted with buffer [50 mM PIPES (pH 6.8) or 50 mM Mes (pH 6.25), both supplemented with 1 mM EGTA, 5 mM EDTA, 0.2 mM $MgCl_2$, 5 mM 2-mercaptoethanol] containing 0.1–1 M KCl. The peak of protein elution was identified by protein assay (at 0.3–0.5 M KCl) and dialysed against either 80 mM PIPES buffer (pH 6.8), 1 mM EGTA, 5 mM EDTA, 0.2 mM $MgCl_2$, 5 mM 2-mercaptoethanol or phosphate buffer (10 mM; pH 7.4). Protein concentration, measured using Advanced Protein Assay Reagent (Cytoskeleton, Inc.) with bovine serum albumin as a standard, was in the range 2.7–4.9 mg/ml. The protein was diluted in phosphate buffer (10 mM; pH 7.4) at a range of concentrations (100–400 μM) for further analysis.

Methylthioninium chloride

Methylthioninium chloride (MTC) was provided by TauRx Therapeutics Ltd. The concentrations are expressed as free MT base.

Assembly of dGAE and incubation with MT

dGAE (100 μM) was incubated at 37 °C with agitation at 700 oscillations per minute (Thermomixer C; Epppendorf, Germany) in the presence of MT at different molar ratios of dGAE to MT (1:0.1, 1:0.5, 1:1, 1:2, 1:5 and 1:10) for 24 h. To investigate the inhibition of dGAE and C322A variant assembly by MT under reducing conditions, samples were incubated either with or without DTT (10 mM) prior to agitation. The assembly process was monitored using CD

spectrometry, negative stain transmission electron microscopy (TEM), X-ray fiber diffraction, and SDS-PAGE.

To investigate the minimal molar ratio required for inhibition, dGAE (100 μM) was incubated using the same assembly conditions in the presence of MT at different molar ratios of dGAE/MTC (1:0.02, 1:0.05, 1:0.1, 1:0.2, 1:0.4, 1:0.6, 1:0.8 and 1:1) for 24 h under reducing conditions.

TEM

Electron microscopy grids were prepared by placing 4 μl of sample onto Formvar®/carbon-coated 400-mesh copper grids (Agar Scientific), blotting excess and then washing with 4 μl of 0.22 μM filtered milli-Q water. Uranyl acetate (4 μl of 2% w/v) was placed on the grid once for 1 minute and then blotted and the grid allowed to air-dry. TEM projection images were collected using a JEOL JEM1400-Plus Transmission Electron Microscope operated at 120 kV equipped with a Gatan OneView camera (4k × 4k). Images were recorded at 25 fps with drift correction using GMS3.

Immunogold labeling TEM

For all dilutions of antibodies and secondary gold probes, a modified phosphate-buffered saline (PBS; pH 8.2) was used; this buffer was supplemented with BSA (1%), Tween-20 (0.005%), 10 mM Na EDTA and NaN_3 (0.2 g/l). dGAE-C322A (100 μM) was incubated with and without MT (10 μM) and incubated for 24 h at 37 °C with agitation at 700 oscillations per minute in the dark. Preformed fibrils were decorated "on grid" using a polyclonal anti-tau antibody (Sigma-Aldrich, SAB4501831). In summary, 4 μl of dGAE-C322 fibrils was pipetted onto Formvar®/carbon-coated 400-mesh copper TEM support grids (Agar Scientific, Essex, UK) and left for 1 min, then a filter paper was used to remove the excess. Normal goat serum (1.10 in PBS, pH 8.2) was used for blocking for 15 min at room temperature. Grids were then incubated with (10 μg/ml IgG) rabbit anti-tau polyclonal antibody for 2 h at room temperature, rinsed three times for 2 min using PBS (pH 8.2), and then immunolabeled with a 10-nm gold particle-conjugated goat anti-rabbit IgG secondary probe (GaR10 British BioCell International, Cardiff, UK; 1.10 dilution) for 1 h at room temperature. The grids were then rinsed five times for 2 min in PBS (pH 8.2) and rinsed five times for 2 min in distilled water. Finally, the grids were negatively stained using 0.5% uranyl acetate. As a negative control, Aß42 fibrils were examined using the same protocol.

CD spectrophotometry

CD was performed using a Jasco Spectrometer J715 and spectra collected in triplicate at a maintained temperature of 21 °C. Protein samples (60 μl) were placed into 0.2-mm path length quartz cuvettes (Hellma) and scanned from 180 to 350 nm. Since the CD spectra were dominated by random coil signal, samples were separated by centrifugation at 20,000*g* for 15 min and 4 °C to isolate fibrillar structures from the mixture. CD was then determined on both supernatant and pellet fractions (40 μl) separately. CD data were presented in mdeg as the protein concentration is unknown and was not possible to measure due to interference of MT and DTT in standard protein assays.

NanoDrop UV–vis spectroscopy

UV–vis spectra were collected for 100 μM MT, 100 μM MT with 50 mM DTT (all prepared in 10 mM PB, pH 7.4) and 10 mM DTT. NanoDrop spectrophotometry was used.

UV/vis and mass spectrometry

Volumetric solutions of MTC (1 mM, 100 μM and 10 μM) and DTT (10 mM; Sigma Aldrich) were prepared in phosphate buffer (pH 7.4, 10 mM; Merck). In addition, volumetric solutions of MTC (1 mM) were prepared in water, phosphate buffer (10 mM) without DTT, and with DTT (10 mM) in water without PB. Solutions were left a minimum of 1.5 h prior to analysis but were observed to be stable for at least 48 h. UV spectrometry was conducted on an Evolution 220 spectrophotometer (Thermo Scientific) running Insight software (version 1.4.40). HRMS data were collected on a Xevo G2-QTof (Waters) running MassLynx software (version 4.1).

SDS-PAGE

SDS-PAGE was conducted on the entire assembly mixtures as well as the supernatant and pellet fractions used for CD (3 μl of each per lane). Samples were mixed with SDS-PAGE sample buffer (without reducing agent) and separated using Any kDa™ Mini-Protean® TGX™ Precast gels (Bio-Rad) at 120 V, until the sample buffer reached the end of the gel. The gel was stained using Imperial Protein Stain (Thermo Scientific), following the manufacturer's instructions, before sealing the gel and scanning on a Canon ImageRunner Advance 6055i scanner.

Acknowledgments

TEM work was performed at the School of Life Sciences TEM Imaging Centre at the University of Sussex, which is supported by the Wellcome Trust and RM Phillips.

S.P. and A.R. are supported by a Sussex Neuroscience doctoral training centre. L.C.S. is supported by Alzheimer's Society and Alzheimer's Research UK Southcoast Network. Y.A., J.R., T.B. and M.S. are supported by TauRx Therapeutics Ltd. C.H., J.S. and C.W. serve as officers in TauRx Therapeutics Ltd.

Appendix A. Supplementary data

Supplementary data to this article can be found online at https://doi.org/10.1016/j.jmb.2018.08.010.

Received 1 June 2018;
Received in revised form 12 July 2018;
Accepted 9 August 2018
Available online 16 August 2018

Keywords:
tau protein;
methylthioninium;
hydromethylthionine;
neurofibrillary tangles;
circular dichroism

Abbreviations used:
AD, Alzheimer's disease; CD, circular dichroism; LMT, leuco-methylthioninium; LMTM, leuco-methylthioninium bis (hydromethanesulfonate); MT, methylthioninium; MTC, Methylthioninium chloride; PBS, phosphate-buffered saline; PHFs, paired helical filaments; TEM, transmission electron microscopy.

References

[1] D.W. Cleveland, S.Y. Hwo, M.W. Kirschner, Physical and chemical properties of purified tau factor and the role of tau in microtubule assembly, J. Mol. Biol. 116 (1977) 227–247.
[2] M. Goedert, M.G. Spillantini, Propagation of Tau aggregates, Mol. Brain 10 (2017) 18.
[3] M.D. Weingarten, A.H. Lockwood, S.Y. Hwo, M.W. Kirschner, A protein factor essential for microtubule assembly, Proc. Natl. Acad. Sci. U. S. A. 72 (1975) 1858–1862.
[4] A. Micsonai, F. Wien, L. Kernya, Y.H. Lee, Y. Goto, M. Refregiers, et al., Accurate secondary structure prediction and fold recognition for circular dichroism spectroscopy, Proc. Natl. Acad. Sci. U. S. A. 112 (2015) E3095–E3103.
[5] C.M. Wischik, M. Novak, P.C. Edwards, A. Klug, W. Tichelaar, R.A. Crowther, Structural characterization of the core of the paired helical filament of Alzheimer disease, Proc. Natl. Acad. Sci. U. S. A. 85 (1988) 4884–4888.
[6] R. Jakes, M. Novak, M. Davison, C.M. Wischik, Identification of 3- and 4-repeat tau isoforms within the PHF in Alzheimer's disease, EMBO J. 10 (1991) 2725–2729.
[7] A.W.P. Fitzpatrick, B. Falcon, S. He, A.G. Murzin, G. Murshudov, H.J. Garringer, et al., Cryo-EM structures of tau filaments from Alzheimer's disease, Nature 547 (2017) 185–190.
[8] B. Falcon, W. Zhang, A.G. Murzin, G. Murshudov, H.J. Garringer, R. Vidal, et al., Structures of filaments from Pick's disease reveal a novel tau protein fold, Nature 561 (2018) 137–140.
[9] N. Okamura, S. Furumoto, M.T. Fodero-Tavoletti, R.S. Mulligan, R. Harada, P. Yates, et al., Non-invasive assessment of Alzheimer's disease neurofibrillary pathology using F-18-THK5105 PET, Brain 137 (2014) 1762–1771.
[10] M. Maruyama, H. Shimada, T. Suhara, H. Shinotoh, B. Ji, J. Maeda, et al., Imaging of tau pathology in a tauopathy mouse model and in Alzheimer patients compared to normal controls, Neuron 79 (2013) 1094–1108.
[11] D.T. Chien, S. Bahri, A.K. Szardenings, J.C. Walsh, F. Mu, M.-Y. Su, et al., Early clinical PET imaging results with the novel PHF-tau radioligand [F-18]-T807, J. Alzheimers Dis. 34 (2013) 457–468.
[12] E.B. Mukaetova-Ladinska, F. Garcia-Sierra, J. Hurt, H.J. Gertz, J.H. Xuereb, R. Hills, et al., Staging of cytoskeletal and β-amyloid changes in human isocortex reveals biphasic synaptic protein response during progression of Alzheimer's disease, Am. J. Pathol. 157 (2000) 623–636.
[13] E. Grober, D. Dickson, M.J. Sliwinski, H. Buschke, M. Katz, H. Crystal, et al., Memory and mental status correlates of modified Braak staging, Neurobiol. Aging 20 (1999) 573–579.
[14] G.K. Wilcock, M.M. Esiri, Plaques, tangles and dementia: a quantitative study, J. Neurol. Sci. 56 (1982) 343–356.
[15] C. Duyckaerts, M. Bennecib, Y. Grignon, T. Uchihara, Y. He, F. Piette, et al., Modeling the relation between neurofibrillary tangles and intellectual status, Neurobiol. Aging 18 (1997) 267–273.
[16] C. Bancher, K. Jellinger, H. Lassmann, P. Fischer, F. Leblhuber, Correlations between mental state and quantitative neuropathology in the Vienna Longitudinal Study on Dementia, Eur. Arch. Psychiatry Clin. Neurosci. 246 (1996) 137–146.
[17] C. Bancher, H. Braak, P. Fischer, K. Jellinger, Neuropathological staging of Alzheimer lesions and intellectual status in Alzheimer's and Parkinson's disease, Neurosci. Lett. 162 (1993) 179–182.
[18] P.W. Arriagada, J.H. Growdon, E.T. Hedley-White, B.T. Hyman, Neurofibrillary tangles but not senile plaques parallel duration and severity of Alzheimer's disease, Neurology 42 (1992) 631–639.
[19] C.M. Wischik, B.O. Schelter, D.J. Wischik, J.M.D. Storey, C.R. Harrington, Modeling prion-like processing of tau protein in Alzheimer's disease for pharmaceutical development, J. Alzheimers Dis. 62 (2018) 1287–1303, https://doi.org/10.3233/JAD-170727.
[20] C.R. Harrington, J.M.D. Storey, S. Clunas, K.A. Harrington, D. Horsley, A. Ishaq, et al., Cellular models of aggregation-dependent template-directed proteolysis to characterize tau aggregation inhibitors for treatment of Alzheimer's disease, J. Biol. Chem. 290 (2015) 10862–10875.
[21] C.M. Wischik, P.C. Edwards, R.Y. Lai, M. Roth, C.R. Harrington, Selective inhibition of Alzheimer disease-like tau aggregation by phenothiazines, Proc. Natl. Acad. Sci. U. S. A. 93 (1996) 11213–11218.
[22] V. Melis, M. Magbagbeolu, J.E. Rickard, D. Horsley, K. Davidson, K.A. Harrington, et al., Effects of oxidized and reduced forms of methylthioninium in two transgenic mouse tauopathy models, Behav. Pharmacol. 26 (2015) 353–368.
[23] A. Crowe, M.J. James, V.M. Lee, A.B. Smith III, J.Q. Trojanowski, C. Ballatore, et al., Aminothienopyridazines and methylene blue affect Tau fibrillization via cysteine oxidation, J. Biol. Chem. 288 (2013) 11024–11037.

[24] Y. Fichou, N.A. Eschmann, T.J. Keller, S. Han, Conformation-based assay of tau protein aggregation, Methods Cell Biol. 141 (2017) 89–112.
[25] C.M. Wischik, M. Novak, H.C. Thøgersen, P.C. Edwards, M.J. Runswick, R. Jakes, et al., Isolation of a fragment of tau derived from the core of the paired helical filament of Alzheimer disease, Proc. Natl. Acad. Sci. U. S. A. 85 (1988) 4506–4510.
[26] E. Akoury, M. Pickhardt, M. Gajda, J. Biernat, E. Mandelkow, M. Zweckstetter, Mechanistic basis of phenothiazine-driven inhibition of Tau aggregation, Angew. Chem. 52 (2013) 3511–3515.
[27] M. Novak, R. Jakes, P.C. Edwards, C. Milstein, C.M. Wischik, Difference between the tau protein of Alzheimer paired helical filament core and normal tau revealed by epitope analysis of monoclonal antibodies 423 and 7.51, Proc. Natl. Acad. Sci. U. S. A. 88 (1991) 5837–5841.
[28] Y.K. Al-Hilaly, S.J. Pollack, D. Vadukul, F. Citossi, J.E. Rickard, M. Simpson, et al., Alzheimer's disease-like paired helical filament assembly from truncated tau protein is independent of disulphide cross-linking, J. Mol. Biol. 429 (2017) 3650–3655.
[29] K. Bhattacharya, K.B. Rank, D.B. Evans, S.K. Sharma, Role of cysteine-291 and cysteine-322 in the polymerization of human tau into Alzheimer-like filaments, Biochem. Biophys. Res. Commun. 285 (2001) 20–26.
[30] A. Iyer, S.J. Roeters, V. Kogan, S. Woutersen, M. Claessens, V. Subramaniam, C-terminal truncated alpha-synuclein fibrils contain strongly twisted beta-sheets, J. Am. Chem. Soc. 139 (2017) 15392–15400.
[31] W.J. Goux, The conformations of filamentous and soluble tau associated with Alzheimer paired helical filaments, Biochemistry 41 (2002) 13798–13806.
[32] R.Y. Lai, C.R. Harrington, C.M. Wischik, Absence of a role for phosphorylation in the Tau pathology of Alzheimer's disease, Biomol. Ther. 6 (2016).
[33] G.K. Wilcock, S. Gauthier, G.B. Frisoni, J. Jia, J.H. Hardlund, H.J. Moebius, et al., Potential of low dose leuco-methylthioninium bis(hydromethanesulphonate) (LMTM) monotherapy for treatment of mild Alzheimer's disease: cohort analysis as modified primary outcome in a phase 3 clinical trial, J. Alzheimers Dis. 61 (2018) 635–657.
[34] R. Brandt, M. Kempf, G. Lee, Expression and purification of Tau for *in vitro* studies, in: J. Avila, R. Brandt, K.S. Kosik (Eds.), Brain Microtubule Associated Proteins: Modifications in Disease, Harwood Academic Publishers, Amsterdam 1997, pp. 245–257.
[35] J.C. Vera, C.I. Rivas, R.B. Maccioni, Heat-stable microtubule protein MAP-1 binds to microtubules and induces microtubule assembly, FEBS Lett. 232 (1988) 159–162.